

IMAGE RECONSTRUCTION TECHNIQUE BASED ON CODED APERTURE IMAGING FOR SuperKEKB X-RAY BEAM SIZE MONITOR

E. Mulyani*, Sokendai, Tsukuba Ibaraki, Japan
 J. Flanagan¹, H. Fukuma¹, H. Ikeda¹, M. Tobiyama¹, KEK, Tsukuba Ibaraki, Japan
¹also at Sokendai, Tsukuba Ibaraki, Japan

Abstract

This paper reports the investigation on the fast reconstruction technique based on principles initially developed for coded aperture imaging, but which have not been applied to accelerator measurements based on coded aperture imaging yet (e.g., at CESR-TA and Diamond Light Source). The establishment of this technique will be necessary for measuring the beam sizes of all 2500 bunches in the SuperKEKB accelerator over thousands of turns, as needed for instability studies and luminosity tuning, due to the vast quantity of data that needs to be processed in a timely manner.

INTRODUCTION

In the SuperKEKB collider, the beam size must be precisely measured, as this plays an essential role in determining the luminosity. Various techniques have been used to measure the beam size such as synchrotron radiation (SR) an interferometer and X-ray imaging with a pinhole camera. We have previously described [1-4] the SuperKEKB x-ray beam size monitor (XRM), which images synchrotron radiation from a bending magnet through an optical element onto a 141- μm -thick YAG:Ce scintillator with a CCD camera as an imaging system. Separate installation of XRM exists for electron (7 GeV High Energy Ring, HER) and positron (4 GeV Low Energy Ring, LER). The optical element is placed at 10.26 (9.47) m from the x-ray source point, and the detector is placed 32.69 (31.79) m from the optical element in the electron (positron) installation; the magnification is 3.186 (3.358). The simplified schematic of the XRM beamline is shown in Fig. 1.

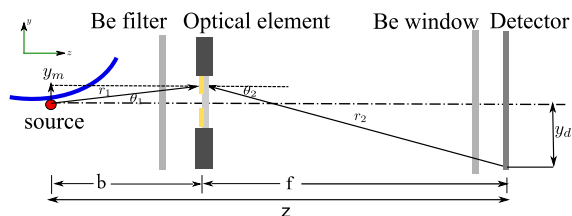


Figure 1: Schematic of the XRM beamline (not to scale).

In the next phase, we will replace the YAG:Ce scintillator with 128 channels of silicon with 2-mm sensing depth and a pixel pitch of 50 μm , with the aim to provide high-resolution bunch-by-bunch, turn-by-turn measurements for low emittance tuning, collision tuning, and instability measurements. In the current phase, we are using the template-fitting method that has excellent capability in the reconstruction of the image source, but in the future, for a single-bunch measure-

ment this method cannot keep up with the vast volumes of data in real-time. We are investigating a fast reconstruction method based on coded aperture (CA) imaging for XRM. This method is important for measuring the beam sizes of all 2500 bunches in the SuperKEKB accelerator over thousands of turns, as needed for instability studies and luminosity tuning.

MATHEMATICAL FORMULATION OF CODED APERTURE IMAGING

Coded aperture imaging is a technique well developed among x-ray astronomers [5] which can, due to higher X-ray collection efficiency, improve on the spatial resolution of a pinhole camera. In astronomy applications, the object is typically 2-dimensional while the XRM is a 1-dimensional device. We consider the geometrical optics of the CA as shown in Fig. 1, where \mathbf{r}_o , b , and f are the source position, source-to-mask distance, and mask-to-detector distance, respectively, the number of counts recorded at the detector position \mathbf{r}_i is given by [6]:

$$R(\mathbf{r}_i) \propto \iint_{\mathbf{r}_o} O(\mathbf{r}_o) A\left(\frac{b}{z}\mathbf{r}_i + \frac{f}{z}\mathbf{r}_o\right) \cos^3(\theta) d^2\mathbf{r}_o, \quad (1)$$

where $\theta = \arctan(|\mathbf{r}_i - \mathbf{r}_o|/z)$ characterizes the trajectories of skew rays through the system, O is the distribution of the object plane, and A is the transmission of the aperture (at the mask plane). If we define

$$\xi = -\frac{f}{b}\mathbf{r}_o, O'(\mathbf{r}) = O\left(\frac{-b}{f}\mathbf{r}\right), \text{ and } A'(\mathbf{r}) = A\left(\frac{-b}{z}\mathbf{r}\right), \quad (2)$$

we can obtain the form

$$R(\mathbf{r}_i) \propto \iint_{\xi} O'(\xi) A'(\mathbf{r}_i - \xi) \times \cos^3\left[\arctan\left(\frac{|\mathbf{r}_i + \frac{b}{f}\xi|}{z}\right)\right] d^2\xi. \quad (3)$$

Here O' and A' are, respectively, rescaled and reflected forms of the object and aperture. The scaling coefficient for O' is the magnification of the pinhole camera (the negative sign indicates that the object is inverted), whereas the scaling coefficient for A' is the ratio of the size of the mask to the size of its projection on the detector. In the far-field approximation, i.e., the object is sufficiently far from the mask and detector, the rays coming from the same point source in the object can be considered parallel so that $\cos^3(\theta) \cong 1$. Under

* mulyani@post.kek.jp

this approximation, the relation in Eq. 3 is reduced to convolution [7], which is the correlation of the rescaled object with the rescaled mask:

$$R(\mathbf{r}_i) \propto \iint_{\xi} O'(\xi)A'(\mathbf{r}_i - \xi)d^2\xi, \quad R = O' * A'. \quad (4)$$

If we have an ideal pair of mask and decoding pattern (A,G) , i.e., a pair such that $A \otimes G = \delta$, then the reconstructed image \hat{O} is defined as [7]:

$$\begin{aligned} \hat{O} &= (O' * A') \otimes G' = \Re[O' * (G' \otimes A')] \\ &= \Re(O' * \delta) = \Re(O'). \end{aligned} \quad (5)$$

where \Re is reflection operator. The reconstructed object is the object itself apart from a rescaling constant.

CODED APERTURE IMAGING IN X-RAY BEAM SIZE MONITOR

There are two steps in the coded aperture imaging concept: the first is encoding, and the second is decoding.

Encoding

The encoding is the physical process of projecting of the object through the mask and onto the detector. In the XRM, after passing through an optical element, X-rays from a point source form a diffraction pattern with single or multiple peaks on the detector depending on the pattern of the optical element. This pattern is the point response function (PRF), i.e., the expected X-ray intensity distribution at the image plane for a given X-ray spectrum, beamline geometry, and optical element. As has been described in detail previously [8-9], the expected image at the detector plane is calculated starting from the σ and π components of the complex wavefront amplitude of the component of synchrotron radiation (SR) with angular frequency ω ,

$$\begin{bmatrix} A_{\sigma} \\ A_{\pi} \end{bmatrix}_{(source)} = \frac{\sqrt{3}}{2\pi} \gamma \frac{\omega}{\omega_c} (1 + X^2)(-i) \begin{bmatrix} K_{2/3}(\eta) \\ \frac{iX}{\sqrt{1+X^2}} K_{1/3}(\eta) \end{bmatrix}, \quad (6)$$

Then the wavefronts $A_{\sigma,\pi}$ are propagated through a model of the beamline, taking account of the attenuation and phase shifts due to the various materials and pathlengths along the way, with a Kirchhoff integral over the surface of the mask,

$$\begin{aligned} A_{\sigma,\pi(det)} &= \frac{iA_{\sigma,\pi(source)}}{\lambda} \times \\ &\int_{mask} \frac{t(y_m)}{r_1 r_2} e^{i\frac{2\pi}{\lambda}(r_1+r_2)} \left(\frac{\cos\theta_1 + \cos\theta_2}{2} \right) dy_m, \end{aligned} \quad (7)$$

where $A_{\sigma,\pi(source)}$ is the (angle-dependent) amplitude of the wave at the source point, λ is the wavelength, and y_d , y_m are the vertical coordinates at the detector and mask, respectively. r_1 (r_2) and θ_1 (θ_2) are the distance and angle from the source point to the mask point at y_m (distance and angle from the mask point y_m to the detector point y_d), respectively. $t(y_m)$ is a complex transmission function at the

mask point y_m . The complex transmission is represented as $t(y_m) = T(y_m)e^{i\delta(y_m)}$, where T is the real transmission and δ is the phase shift due to passing through the mask material at y_m . For each pixel in the detector, the wavefront amplitude from each source point is calculated and converted to the detected flux, which is defined as

$$\begin{bmatrix} \frac{d^2 \mathcal{F}_{\sigma}}{d\theta d\psi} \\ \frac{d^2 \mathcal{F}_{\pi}}{d\theta d\psi} \end{bmatrix} = \alpha \frac{\Delta\omega}{\omega} \frac{I}{e} |A_{\sigma,\pi}(\omega)|^2. \quad (8)$$

The weighted flux contributions from source points are then summed over the source distribution. This process is repeated over the detectable spectral range, taking into account the material properties of the detector. By varying the weighting of source points and comparing the resulting image against data, the source Gaussian profile can be reconstructed.

A Uniformly Redundant Array (URA) [7] has been installed in the XRM as an optical element. In a 1-dimensional URA, features are described by a series of cells that either transmitting or opaque. Our URA pattern is 01101100010101100001000001111011110010101110010 (12-slits), 1 and 0 represents the hole (transmitting) and opaque, respectively. The detector is 128 channels of silicon with 2-mm sensing depth and a pixel pitch of 50 μm . Figure 3 shows the simulated detector images for both rings.

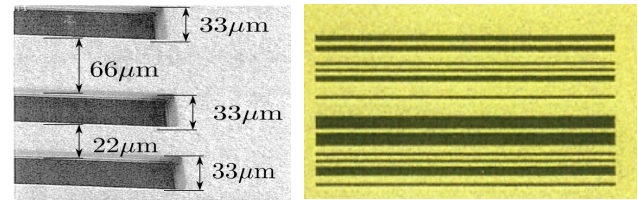


Figure 2: 12-slits URA mask pattern; (left) 1000 \times Scanning Electron Microscope, and (right) consist of 20- μm -thick gold masking material on 600- μm -thick diamond substrates.

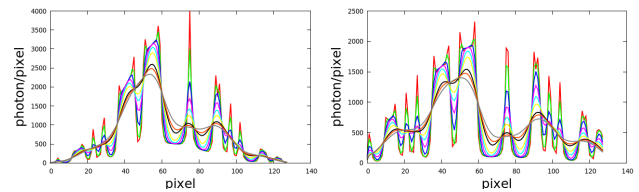


Figure 3: Simulated detector images showing the number of photons/pixel for 1mA in LER (left) and HER (right) with the number of photons for LER and HER are 1943 and 3342 photons/turn/mA/bunch, respectively.

Decoding: computer post-processing

The second step of coded aperture imaging is extracting the encoded data (image reconstruction). Various methods for image reconstruction are possible, direct deconvolution (using Fourier transform, FT) and correlation methods are examples. The straightforward way of performing the image

reconstruction is employing the Fourier transform which reduces a convolution to a simple multiplication. Providing the Fourier transform of each function in Eq. 4 with a noise term N , the estimate \hat{O} is then given by:

$$\hat{O} = \mathcal{F}^{-1}\left(\frac{\mathcal{F}(R)}{\mathcal{F}(A)}\right) = O - \mathcal{F}^{-1}\left(\frac{\mathcal{F}(N)}{\mathcal{F}(A)}\right). \quad (9)$$

The main problem with direct deconvolution methods is that $\mathcal{F}(A)$ might have small terms. The mask aperture A is usually defined as an array of ones and zeros where the ones have the same pattern in the array as do the pinholes in the aperture.

Another method of decoding is suggested by Eqs. 4 and 5 as shown in Eq. 10 where N is a noise term. The choice of the decoding matrix G must be such that $G * A$ is as close as possible to a delta function, to preserve the object features within the system resolution. One method is to use the array A itself as the decoding matrix which is the auto-correlation method [7]:

$$\begin{aligned} \hat{O} &= (O' * A' + N) \times G = (O' * A') \times G + N \times G \\ &= O' * (A' \times G) + N \times G. \end{aligned} \quad (10)$$

If $A' \times G = \delta$ then Eq. 10 becomes $\hat{O} = O' + N \times G$. The noise term is still present but unlike in the Fourier transform method, is not ill-behaved. An improvement over the auto-correlation method process can be obtained by a balanced correlation method [6], that is achieved by using the G array as, $G(i, j) = 1$ if $A(i, j) = 1$ and $G(i, j) = -\rho/(1 - \rho)$ if $A(i, j) = 0$, where ρ is the density of the aperture array. The balanced method is similar to the mismatch method of Brown [10] that defined $G(i, j) = 1$ if $A(i, j) = 1$ and $G(i, j) = -1$ if $A(i, j) = 0$. If the $\rho = 0.5$ the balanced correlation is the same as the Brown mismatch approach; the balanced correlation will work better than the mismatch when ρ is not 0.5 [7].

IMPLEMENTATION

In implementing the coded aperture imaging, we proceed as below:

1. We defined b and f with the beamline arrangement as shown in Fig. 1.
2. The mask aperture A is 12-slits pattern as shown in Fig. 2 with 47 pixels size. The holes occupy $\sim 48\%$ of the aperture then we defined G as $G = 1$ if $A(i, j) = 1$ and $G = -0.917$ if $A(i, j) = 0$
3. We constructed the G pattern, the correlation between A and G is a δ function.
4. The detector is 128 channels of silicon with 2-mm sensing depth and a pixel pitch of 50 μm .
5. The pixel size of the projection image R in the detector is 128, so we need to re-binned it into 47 pixels to make it suitable for G in the deconvolution process.
6. Deconvolution process using the direct convolution (FT) and correlation methods, we consider without noise term.

7. In the case of XRM, the object is a single source with a Gaussian vertical spread. Therefore, we applied Gaussian fitting in the reconstructed image.

The results of decoding using both methods are shown in Fig. 4. The reconstructed image is a Gaussian function with an artifact/sidelobe eventhough the correlation between A and G is a perfect delta function. This artifact could be because the masking region of the image does not entirely block the x-rays, allowing some background to leak through the mask pixels. The other possibility is because we use a far-field approximation in the analysis. The apertures that in far-field ensure artifact-free imaging could deviate significantly from ideal when used in the near-field. As we see in Eq. 1, in the near-field case, there is a $\cos^3\theta$ that we need to take into account.

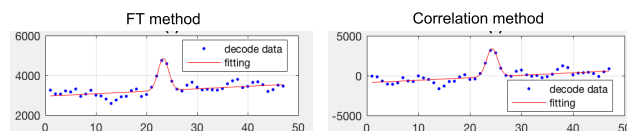


Figure 4: Image reconstruction process using (left) direct deconvolution/FT and (right) correlation methods.

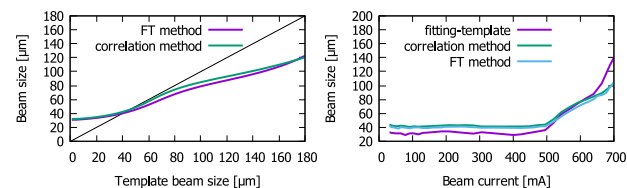


Figure 5: Comparison of CA deconvolution technique and fitting-template method.

During the phase I of SuperKEKB commissioning (Spring 2016), we collected data of beam size as a function of beam current using the fitting-template method. Figure 5 shows the comparison of CA deconvolution technique and fitting-template method. For beam size smaller than 80 μm (Fig. 5(left)), the result is reasonable. For large beam sizes, there is a significant deviation compared to the template beam size. One reason is the difficulty in Gaussian fitting, especially at large beam sizes. This difficulty could be because of the artifact that appears as we mentioned before. In Fig. 5(right), there is a small deviation between CA deconvolution and fitting-template at the lower beam current (less than 500 mA). At the beam current less than 500 mA, the raw beam size is around 38 – 41 μm . The point-spread function (PSF) of the single slit (33 μm) when the detector (Si) sees it is ~ 34 μm , then we would not be able to see the raw beam size smaller than the PSF.

CONCLUSION

We are investigating the reconstruction technique based on coded-aperture imaging for X-ray beam profile monitoring to measure bunch-by-bunch profiles. In the far-field approximation, we can reconstruct the point source and comparable with the template-fitting method especially at the

small beam size (less than 80 μm). In further analysis, we need to take into account the near-field approximation to reduce the artifact in the reconstructed image. We also will study the fitting-method for the simulated detector image and compare it with the phase I data result.

REFERENCES

- [1] *SuperKEKB Design Report*, KEK Technical Report, 2014.
- [2] J. W. Flanagan *et al.*, in *Proc. of 7th Annual Meeting of Particle Accelerator Society of Japan.*, 2010, pp. 618–622.
- [3] E. Mulyani and J. W. Flanagan, in *Proc. of IBIC'15*, Melbourne, pp. 377–380.
- [4] E. Mulyani and J. W. Flanagan, in *Proc. of IBIC'16*, Barcelona, pp. 524–527.
- [5] R. H. Dicke, in *The Astrophysical Journal*, 1968, vol. 153.
- [6] R. Accorsi and R. Lanza, in *Journal of Applied Optics (OSA)*, vol. 40, No. 26, 2001, pp. 4698–4705.
- [7] E. E. Fenimore and T. M. Cannon, in *Journal of Applied Optics (OSA)*, vol. 17, 1961. pp. 337–347.
- [8] J. W. Flanagan *et al.*, in *Proc. of DIPAC'11*, pp. 561–563.
- [9] J. W. Flanagan *et al.*, in *Proc. of IPAC'10*, pp. 966–968.
- [10] C. M. Brown, “Multiplex imaging and random array”, Ph.D. thesis, U. Chicago, 1972.